www.czasopisma.pan.pl PAN POLSKA AKADEMIA NAUK www.journals.pan.pl

VERSITA

Arch. Min. Sci., Vol. 58 (2013), No 3, p. 655–672

Electronic version (in color) of this paper is available: http://mining.archives.pl

DOI 10.2478/amsc-2013-0046

H. MOLLADAVOODI*

STUDY OF GROUND RESPONSE CURVE (GRC) BASED ON A DAMAGE MODEL

BADANIE KRZYWEJ ODPOWIEDZI GRUNTU (GRC) W OPARCIU O MODEL PĘKANIA SKAŁ

Analysis of stresses and displacements around underground openings is necessary in a wide variety of civil, petroleum and mining engineering problems. In addition, an excavation damaged zone (EDZ) is generally formed around underground openings as a result of high stress magnitudes even in the absence of blasting effects. The rock materials surrounding the underground excavations typically demonstrate nonlinear and irreversible mechanical response in particular under high in situ stress states. The dominant cause of irreversible deformations in brittle rocks is damage process.

One of the most widely used methods in tunnel design is the convergence-confinement method (CCM) for its practical application. The elastic-plastic models are usually used in the convergence-confinement method as a constitutive model for rock behavior. The plastic models used to simulate the rock behavior, do not consider the important issues such as stiffness degradation and softening. Therefore, the use of damage constitutive models in the convergence-confinement method is essential in the design process of rock structures. In this paper, the basic concepts of continuum damage mechanics are outlined. Then a numerical stepwise procedure for a circular tunnel under hydrostatic stress field, with consideration of a damage model for rock mass has been implemented. The ground response curve and radius of excavation damage zone were calculated based on an isotropic damage model. The convergence-confinement method based on damage model can consider the effects of post-peak rock behavior on the ground response curve and excavation damage zone. The analysis of results show the important effect of brittleness parameter on the tunnel wall convergence, ground response curve and excavation damage radius.

Keywords: rock damage, constitutive model, damage mechanics, convergence-confinement method, Strain Softening

Analiza naprężeń i przemieszczeń powstałych wokół otworu podziemnego wymagana jest przy szerokiej gamie projektów z zakresu budownictwa lądowego, inżynierii górniczej oraz naftowej. Ponadto, wokół otworu podziemnego powstaje strefa naruszona działalnością górniczą wskutek oddziaływania wysokich naprężeń, nawet w przypadku gdy nie są prowadzone prace strzałowe. Reakcja materiału skalnego znajdującego się w otoczeniu wyrobisk podziemnych jest zazwyczaj procesem nieliniowym i nieodwracalnym, zwłaszcza w stanach wysokich naprężeń in situ. Główną przyczyną nieodwracalnych odkształceń skał kruchych jest pękanie.

* DEPARTMENT OF MINING AND METALLURGICAL ENGINEERING, AMIRKABIR UNIVERSITY OF TECHNOLOGY, TEHRAN, IRAN. E-MAIL ADDRESS: hamedavodi@aut.ac.ir.

Jedną z najczęściej stosowanych metod w projektowaniu tuneli (wyrobisk podziemnych) jest metoda konwergencji i zamknięcia, popularna ze względu na zakres zastosowań. Metoda ta zazwyczaj wykorzystuje modele sprężysto- plastyczne, jako konstytutywne modele zachowania skał. Modele plastyczne wykorzystywane dotychczas do symulacji zachowania skał nie uwzględniają pewnych kluczowych aspektów, takich jak obniżenie sztywności czy rozmiękczanie. Dlatego też zastosowanie konstytutywnych modeli w metodzie konwergencji i zamknięcia jest sprawą kluczową przy projektach obejmujących struktury skalne. W pracy tej omówiono podstawowe założenia modelu continuum uszkodzeń i spękań. Zaimplementowano wielostopniową procedurę do badania tunelu o przekroju kolistym znajdującego się pod polem naprężeń hydrostatycznych, przy wykorzystaniu modelu pękania górotworu. Krzywą odpowiedzi gruntu oraz promień strefy naruszonej wybieraniem obliczono przy wykorzystaniu izotropowego modelu uszkodzeń. Metoda konwergencji i zamykania oparta na tym modelu uwzględnia zachowanie skał po wystąpieniu szczytowych naprężeń i powstaniu strefy naruszonej wybieraniem. Analiza wyników wykazała znaczny wpływ parametrów związanych z kruchością na konwergencję ścian wyrobiska, kształt krzywej odpowiedzi gruntu oraz promień strefy naruszonej wybieraniem.

Słowa kluczowe: pękanie skał, model konstytutywny, mechanika spękań, metoda konwergencji i zamknięcia, uplastycznienie

1. Introduction

The convergence confinement method (CCM) is an effective analytical tool for the underground openings design. It consists of three basic components: longitudinal deformation profile (LDP), support characteristic curve (SCC) and ground response curve (GRC). The study of the interaction between support and tunnel can easily be carried out using the convergence-confinement method. The GRC, which describes the relationship between decreasing of inner support pressure and the increasing of radial displacement of tunnel wall, is generally evaluated by analytical methods based on axial symmetry plane strain assumption (Guan et al., 2007).

Many studies have been conducted on the tunnel convergence-confinement method. These available studies, although distinguished from different failure criterions and post-failure behaviors, are generally based on the plasticity theory (Brown et al., 1983; Oreste & Peila, 1996; Jiang et al., 2001; Detournay, 1986; Carranza-Torres & Fairhurst, 1999; Alonso et al., 2003).

The dominant causes of irreversible deformations are plastic flow and damage process. The plastic flow is controlled by the presence of local shear stresses which cause dislocation to some preferential elements due to existing defects. During this process, the net number of bonds remains practically unchanged. The overall macroscopic consequence of plastic flow is that the elastic properties and, therefore, the stiffness of the material are insensitive to this type of irreversible change (Yazdani & Schreyer, 1988). The main cause of irreversible changes in quasi brittle materials such as rock is the damage process occurring within the material. From a microscopic viewpoint, damage initiates with the nucleation and growth of microcracks. When the microcracks length reaches a critical value, the coalescence of microcracks occurs and localized meso-cracks appear (Shao et al., 2006).

The macroscopic and phenomenological consequence of damage process is stiffness degradation, dilatation, & softening (Molladavoodi & Mortazavi, 2010). In this paper, the ground reaction curve (GRC) was formulated based on the damage mechanics theory.

The construction of a long circular tunnel under a hydrostatic in situ stress condition can be considered as an axial symmetry plane strain problem. After tunnel excavation, the surrounding rock mass behaves elastic and softening sequentially.

According to different fictitious inner pressure provided by the tunnel face and the support, elastic and damage zone will be created around the tunnel. Fig. 1 shows a circular tunnel being

excavated in a continuous, homogeneous, isotropic, initially elastic rock mass subjected to a hydrostatic stress P_0. The tunnel surface is subjected to an internal pressure P_i. As P_i is gradually reduced, the radial displacement occurs and a damage zone develops around the tunnel when P_i is less than the yield stress.

In Fig. 1, P_0 is the hydrostatic in situ stress; a & R_d are the radii of the tunnel and the elastic-softening interface respectively.

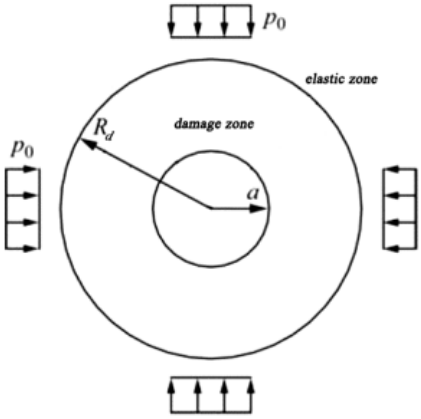

Fig. 1. Schematic representation of the rock mass zones after tunnel excavation

The main objective of this paper is to develop a procedure for obtaining the ground response curve of a circular tunnel excavated in elastic-damage rock mass.

The strength of the rock mass in the strain softening zone must be described properly. In other studies, the rock strength decreases linearly with strain increment. In this model, the rock strength declines as hyperbolic decay similar to the experimental observations.

2. A Damage Constitutive Model

In this model, the rock in pre failure region behaves linear elastic. With stress increment, the stress state is attained to the failure criteria. The failure criterion in this model is assumed Mohr-Coulomb failure criterion as following:

$$F = \sigma_1 - k_\phi \sigma_3 - f_c(D) = 0 \tag{1}$$

where σ_1, σ_3 are major principal stresses respectively. k_ϕ is the constant frictional coefficient calculated as below:

$$k_\phi = \frac{1+\sin\phi}{1-\sin\phi} \tag{2}$$

In Eq. (1), $f_c(D)$ is resistant function of failure surface depending on the rock damage variable (D). Because of tunnel hydrostatic loading condition, the pre and post failure rock behavior is considered isotropic. In damage mechanics, rock stiffness is gradually degraded by damage progression. The stiffness modulus of damaged rock is calculated based on following relation:

$$E = (1 - D) E_0 \tag{3}$$

where E_0 and E are the rock stiffness modulus of intact and damaged rock respectively. Because of isotropic damage, the rock stiffness modulus in Eq. (3) is scalar. The range of damage variable (D) is between 0 (intact rock) to 1 for completely damaged rock.

After peak strength, the strength of rock drops gradually with increasing strain and follows the softening behavior. In softening region, the rock strength is degraded as power law function with strain increment. The rock stress-strain curve under uniaxial compressive strength is illustrated in Fig. (2).

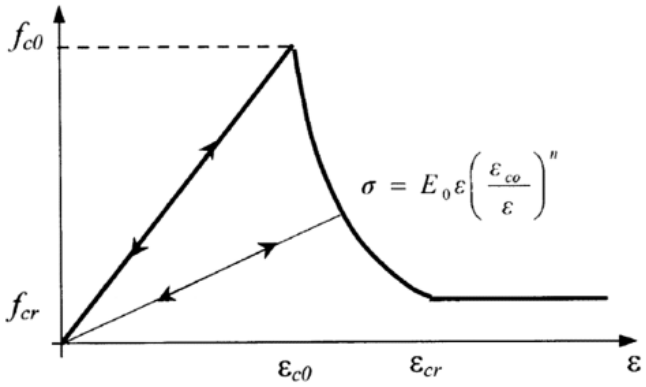

Fig. 2. The rock stress-strain curve with Power-law softening and residual strength at post-peak region (Zhu & Tang, 2004)

The residual strength coefficient (λ) is defined as the fraction of residual (f_{cr}) to peak strength (f_{c0}) (Zhu & Tang, 2004). ε_{c0} is strain at peak strength (f_{co}). In Fig. (2), the post-peak rock stress-strain curve consists of two regions. In first part, the rock strength is decreased as power law softening with strain increment. After the rock strength decreases to residual strength (corresponding to ε_{cr}), it is fixed to residual strength in second region. Based on (Zhu & Tang, 2004), the stress-strain curve in softening region is described with decreasing and power-law relation:

$$\sigma = E_0 \cdot \left(\frac{\varepsilon_{co}}{\varepsilon} \right)^b \cdot \varepsilon \tag{4}$$

where b is rock brittleness parameter. Based on Eq. (4), the strain corresponding to residual strength (ε_{cr}) can be expressed as

$$\varepsilon_{cr} = \frac{\varepsilon_{co}}{\sqrt[(b-1)]{\lambda}} \tag{5}$$

With comparison of Eqs. (3) & (4), the damage evolution rule is explained as below:

$$D = \begin{cases} 0 & \varepsilon < \varepsilon_{c0} \\ 1 - \left(\dfrac{\varepsilon_{co}}{\varepsilon}\right)^{b} & \varepsilon_{co} \le \varepsilon < \varepsilon_{cr} \\ 1 - \dfrac{\lambda \varepsilon_{co}}{\varepsilon_{cr}} & \varepsilon_{cr} \le \varepsilon \end{cases} \tag{6}$$

In above equation, the damage evolution law is defined based on total strain. The shear damage evolution is always related to maximum compressive strain (Zhu & Tang, 2004). Based on tunnel loading status, the tangential strain (ε_θ) is substituted to the uniaxial compressive strain (ε) in Eq. (6). The mechanical behavior of rock in biaxial compression and confinement state of tunnel is associated with increasing of rock strength and strain corresponding to the peak strength. Therefore, the tangential strain at interface of the elastic and damage zone ($\varepsilon_{\theta e}$) can be substituted to ε_{co} in Eq. (6). As a result, Eq. (6) can be rewritten as below:

$$D = \begin{cases} 0 & \varepsilon_\theta < \varepsilon_{\theta e} \\ 1 - \left(\dfrac{\varepsilon_{\theta e}}{\varepsilon_\theta}\right)^{b} & \varepsilon_{\theta e} \le \varepsilon_\theta < \varepsilon_{cr} \\ 1 - \dfrac{\lambda \varepsilon_{\theta e}}{\varepsilon_\theta} & \varepsilon_{cr} \le \varepsilon_\theta \end{cases} \tag{7}$$

Based on Eq. (4), the rock strength (f_c) in softening region is decreased as below

$$f_c = \left(\frac{f_{c0}}{\varepsilon_{\theta e}}\right) \cdot \left(\frac{\varepsilon_{co}}{\varepsilon_\theta}\right)^{b} \cdot \varepsilon_\theta \tag{8}$$

Based on (Molladavoodi & Mortazavi, 2011), the brittleness parameter is defined as following

$$b = \frac{r_0}{g_f - r_0} \tag{9}$$

In above equation, r_0 is elastic energy associated with peak strength (f_{c0}) can be calculated from the following equation:

$$r_0 = \frac{f_{c0}^{\ 2}}{2E_0} \tag{10}$$

In Eq. (9), g_f is the area under the compressive uniaxial stress-strain diagram (compressive fracture energy for unit volume). This rock parameters definition is showed in Fig. (3).

Based on Eq. (9), the relation between the brittleness parameter (b) and the fraction of $\frac{g_f}{r_0}$ is illustrated in Fig. 4.

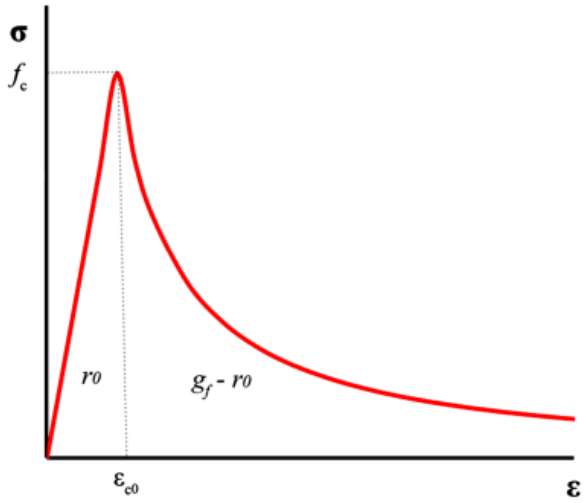

Fig. 3. The definition of elastic strain energy and rock fracture energy

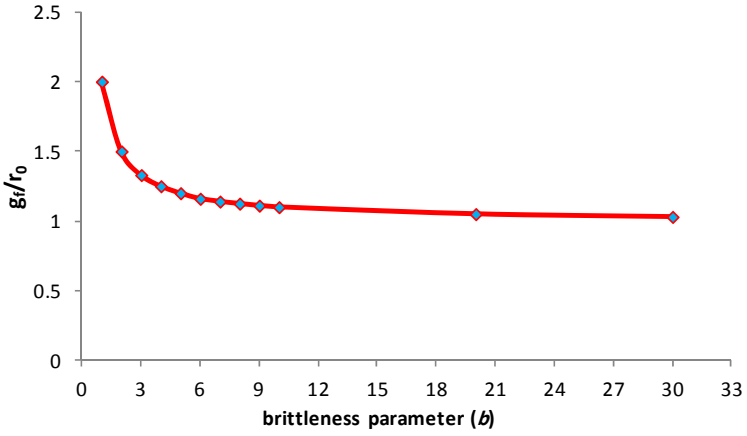

Fig. 4. The relation between the brittleness parameter (b) and the fraction of $\frac{g_f}{r_0}$

As shown in Fig. 4, rock with increase of the brittleness parameter (b) behaves perfectly brittle ($g_f = r_0$). With decrease of the brittleness parameter (b), the ductility of rock post-peak behavior increased.

The relation between minimum and maximum principal strains in elastic zone is defined by Poisson' ratio (v). After microcracks creation and progression in damage zone, the ratio between minimum and maximum principal strains is increased. In damage and residual zones, these relations can be expressed as

$$d\varepsilon_r = d\varepsilon_r^e - f \cdot (d\varepsilon_\theta - d\varepsilon_\theta^e) \tag{11}$$

Based on the isotropic damage mechanics, the parameter (f) within damage zone can be written as (Carol et al., 2001)

$$f = \frac{\upsilon^0}{1-D} \tag{12}$$

where υ^0 is Poisson' ratio of intact rock.

3. Analyses of Ground Responses

3.1. Elastic Zone

The elastic solution for the excavation of cylindrical cavities in a hydrostatically loaded medium is given by Lame' solution (Timoshenko & Goodier, 1970). It applies to the elastic region of this problem (where $r > R_d$). The stress distributions in this region can be expressed as

$$\sigma_r = P_0 - (P_0 - \sigma_{re})\left(\frac{R_d^2}{r^2}\right) \tag{13}$$

$$\sigma_\theta = P_0 + (P_0 - \sigma_{re})\left(\frac{R_d^2}{r^2}\right) \tag{14}$$

where σ_r and σ_θ are the stresses in radial and tangential directions; P_0 is in situ and initial isotropic stress of region, and σ_{re} denotes the radial stress at the elastic-damage interface (R_d). The distributions of radial strains (ε_r), tangential strains (ε_θ), and radial displacement (u) is expressed as below

$$\varepsilon_r = -\frac{(P_0 - \sigma_{re})}{2G_0}\left(\frac{R_d^2}{r^2}\right) \tag{15}$$

$$\varepsilon_\theta = \frac{(P_0 - \sigma_{re})}{2G_0}\left(\frac{R_d^2}{r^2}\right) \tag{16}$$

$$u = \frac{(P_0 - \sigma_{re})}{2G_0}\left(\frac{R_d^2}{r}\right) \tag{17}$$

where G_0 is the shear modulus of intact rock. Since the radial and tangential stresses at the elastic-damage interface ($r = R_d$) should satisfy the Mohr-Coulomb criterion in Eq. (1), it leads to

$$\sigma_{re} = \frac{2P_0 - f_{c0}}{k_\phi + 1} \tag{18}$$

$$\sigma_{\theta e} = 2P_0 - \frac{2P_0 - f_{c0}}{k_\phi + 1} \tag{19}$$

Based on Eqs. (17) & (18), the radial and tangential strains at the elastic and damage zones interface ($r = R_d$) can be calculated as below

$$\varepsilon_{re} = -\frac{\left(P_0 - \sigma_{re}\right)}{2G_0} \tag{20}$$

$$\varepsilon_{\theta e} = \frac{\left(P_0 - \sigma_{re}\right)}{2G_0} \tag{21}$$

3.2. Damage Zone

It is required to solve for the stresses and displacements in the damage zone to obtain the ground response curve. Assuming a state of plane strain and axial symmetry around the tunnel opening, the strain-displacement compatibility equation in polar coordinate system can be expressed as

$$\varepsilon_\theta = \frac{u}{r}, \quad \varepsilon_r = \frac{du}{dr} \tag{22}$$

Because of the complex stress-strain relation in damage zone, it not possible to find closed-form solutions to the stress and strain distributions. In this condition, a numerical solution proposed by Brown et al. (1983) was used. This numerical solution includes a stepwise procedure that calculates the stresses, strains, and displacements on the boundaries of a number of annular rings. The damage zone is divided to a number of annular rings. Based on Fig. 5 , ring $(j-1)$ lies between normalized radii $\rho_{(j)} = r_{(j)}/R_d$ and $\rho_{(j-1)} = r_{(j-1)}/R_d$. The displacement, strain, and stress at the normalized radius $\rho_{(j)}$ can be written as $u_{(j)}$, $\varepsilon_{0(j)}$, $\varepsilon_{r(j)}$, $\varepsilon_{0(j)}$ and $\sigma_{r(j)}$.

Based on Eq. (24) and damage zone division to annular rings, the strain-displacement relations at normalized radii $\rho_{(j)}$ and $\rho_{(j-1)}$ is as following

$$\varepsilon_{\theta(j)} = \frac{u_{(j)}}{\rho_{(j)}}, \quad \varepsilon_{r(j)} = \left(\frac{du}{d\rho}\right)_j \tag{23}$$

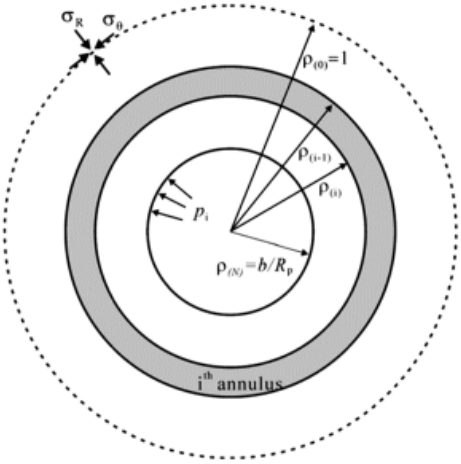

Fig. 5. Normalized damage zone with finite number of annuli (Lee & Pietruszczak, 2008)

If the annular rings are considered quite thin, an approximate relation can be written as below

$$\frac{u_{(j-1)}-u_{(j)}}{\rho_{(j-1)}-\rho_{(j)}}=\frac{1}{2}\left[\left(\frac{du}{d\rho}\right)_{(j-1)}+\left(\frac{du}{d\rho}\right)_{(j)}\right] \tag{24}$$

If the displacement expression and its derivative calculated by Eq. (25) is substituted in above equation, Eq. (26) can be rewritten as

$$\rho_{(j)}=\frac{2\varepsilon_{\theta(j-1)}-\varepsilon_{r(j-1)}-\varepsilon_{r(j)}}{2\varepsilon_{\theta(j)}-\varepsilon_{r(j-1)}-\varepsilon_{r(j)}}\cdot\rho_{(j-1)} \tag{25}$$

In a step of numerical calculation, the tangential strain (ε_θ) increased as $d_{\varepsilon\theta}$. The tangential strain increment ($d_{\varepsilon\theta}$) selected an arbitrary small value. The tangential strain increment is as below

$$d\varepsilon_\theta=\varepsilon_{\theta(j)}-\varepsilon_{\theta(j-1)} \tag{26}$$

In the strain-softening region, the radial strain increment at $\rho_{(j)}$ can be calculated as following

$$d\varepsilon_{r(j)}=d\varepsilon^e_{r(j-1)}-f\cdot(d\varepsilon_{\theta(j)}-d\varepsilon^e_{\theta(j-1)}) \tag{27}$$

where $\varepsilon^e_{r(j-1)}$, $d\varepsilon^e_{\theta(j-1)}$ are the radial and circumferential elastic strain increments at $\rho_{(j-1)}$ respectively. The elastic strains at $\rho_{(j-1)}$ can be calculated by using the elastic stress-strain relationship

$$\varepsilon^e_{r(j-1)}=\frac{1}{2G}\left[(1-\nu)\left(\sigma_{r(j-1)}-P_0\right)-\nu\left(\sigma_{\theta(j-1)}-P_0\right)\right] \tag{28}$$

$$\varepsilon^{e}_{\theta(j-1)} = \frac{1}{2G}\left[(1-\nu)\left(\sigma_{\theta(j-1)} - P_0\right) - \nu\left(\sigma_{r(j-1)} - P_0\right)\right] \tag{29}$$

where G is shear modulus of the rock (Park et al., 2008).

The parameter (f) is calculated based on Eq. (14). At elastic-damage boundary ($\rho = \rho_{(1)} = 1$), the principals strains ($\varepsilon_{\theta(1)}, \varepsilon_{r(1)}$) are given by Eqs. (22) & (23). $\varepsilon_{\theta(2)}, \varepsilon_{r(2)}$, and $\rho_{(2)}$ can be calculated using an arbitrary small value ($d_{\varepsilon\theta}$) and based on Eqs. (27), (28), and (29). With increment of tangential strain, the damage variable increased and the rock strength decreased based on Eqs. (7) & (8) respectively. Then the parameter (f) is estimated based on the updated damage variable.

The stress states in the softening region should satisfy the Mohr-Coulomb failure criterion. Because of the axial symmetry of the problem, the failure criterion can be expressed with the radial and circumferential stresses, σ_r and σ_θ, such as

$$F = \sigma_\theta - k_\phi \sigma_r - f_c = 0, \qquad \sigma_\theta = k_\phi \sigma_r + f_c \tag{30}$$

The differential equation of equilibrium must be satisfied by the rock stress state as below

$$\frac{d\sigma_r}{d\rho} + \frac{\sigma_r - \sigma_\theta}{\rho} = 0 \tag{31}$$

In above equation, the tangential stress (σ_θ) is substituted from Eq. (32). It leads to

$$\frac{d\sigma_r}{d\rho} + \frac{\left(1-k_\phi\right)\sigma_r + f_c}{\rho} = 0 \tag{32}$$

By dividing the damage zone with a number of thin annular rings (Fig. 4), the above equation can be rewritten between normalized radii $\rho_{(j-1)}$ and $\rho_{(j)}$ as following

$$\frac{\sigma_{r(j)} - \sigma_{r(j-1)}}{\rho_{(j)} - \rho_{(j-1)}} + \frac{\left(1-k_\varnothing\right)\left[\dfrac{\sigma_{r(j)} + \sigma_{r(j-1)}}{2}\right] + f_{c(j)}}{\left[\dfrac{\rho_{(j-1)} + \rho_{(j)}}{2}\right]} = 0 \tag{33}$$

After some manipulation on above equation, the solution for $\sigma_{r(j)}$ is as below

$$\sigma_{r(j)} = \sigma_{r(j-1)} - 2\left(\frac{\rho_{(j-1)} - \rho_{(j)}}{2\rho_{(j)} + k_\phi\left(\rho_{(j-1)} - \rho_{(j)}\right)}\right) \cdot f_{c(j)} \tag{34}$$

where $f_{c(j)}$ is the post-peak rock strength can be calculated based on Eq. (8).

The radial stress on the outer boundary of the first annulus in which ($\rho = \rho_{(1)} = 1$) is given by Eq. (20). Using this as the starting point, successive values of $\sigma_{r(j)}$ may be calculated from

Eq. (36) for the normalized radii determined from Eq. (27). When ε_θ reaches the residual strain (ε_{cr}) on Eq. (5), the rock strength is considered constant at the residual strength (f_{cr}).

The stepwise process was repeated several times to determine completely the stresses, strains, and displacements in damage and residual zones. After n times calculation, the last $\sigma_{r(j)}$, i.e. $\sigma_{r(n)}$, reaches the internal support pressure value, P_i which is acting on the excavation surface of the opening with radius a. The damage radius R_d can be obtained from the following relation:

$$R_d = \frac{a}{\rho_{(n)}} \tag{35}$$

The convergence of the tunnel wall can be calculated as below

$$u_{(n)} = \varepsilon_{\theta(n)} \cdot a \tag{36}$$

It is obvious that the solution will converge to the exact solution by increasing the division number n. This calculation procedure can be easily implemented into the computer program to obtain the ground response curve.

4. Application

In order to show the applicability of the proposed damage model in evaluation of the ground reaction curve and excavation damage zone, a typical circular tunnel of radius $a = 5$ m is considered. This tunnel is excavated in a fair to good quality rock at depth which the in situ hydrostatic stress is $P_0 = 55$ MPa. Table 1 shows the rock mass properties used to solution. Similar conditions could exist in the deep tunnel projects.

TABLE 1

The rock mass properties used to solution

E_0 (GPa)	v	Ø	f_{c0} (MPa)	λ	Brittleness (b)
30	0.22	25	50	0.1	1-3

This problem was solved assuming that the idealized rock mass behavior shown in Fig. 2 applies to the rock mass. A principal strain increment of $d\varepsilon_{\theta(j)} = 0.01\varepsilon_{\theta(j-1)}$ was used in Eqs. 28 & 29.

4.1. Ground response curves and excavation damage radius

The ground response curve and excavation damage radius were calculated based on the damage model and numerical stepwise procedure presented in section 3 and Appendix. Fig. 6 shows ground response curves (GRC) at different brittleness parameters (b).

The internal support pressure (P_i) on tunnel wall decreases in Fig. 6. With decrease of fictitious inner support pressure (P_i), the tunnel wall convergence increases. Fig. 6 shows important effect of brittleness parameter (b) on ground response curves (GRC). The initial parts of all ground response curves with different brittleness parameters are same. The primary sections of GRCs are

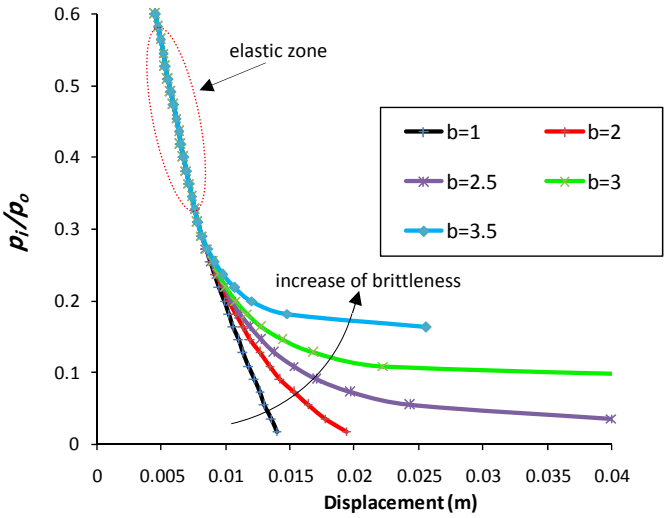

Fig. 6. Ground response curves at different brittleness parameters

relevant to the elastic behavior so they are not dependent on the brittleness parameter (b). The second sections of ground response curves are related to the damage zone so there is a bifurcation point on this section of the ground response curves (GRCs) after elastic behavior. Because of different brittleness parameters used in ground response curves analysis, the ground response curves are not similar in damage zone. It is evident in Fig. 6 that the tunnel wall convergence increases with brittleness parameter (b) increment. In a brittle rock exhibiting rapid loss strength with strain increment, the capacity of absorbed fracture energy at post-peak region decreases so the tunnel wall convergence increases. Therefore, the tunnel wall convergence in a much more brittle rock is more than a much less brittle rock if other rock strength properties are same.

The results for $b = 1$ show that the tunnel wall convergence is small even though without internal support pressure ($P_i = 0$). The calculations indicate that the tunnel will stabilize at $b = 1$ & 2 following some displacements. However, the results for $b = 3$ & 3.5 illustrate that the tunnel wall convergence is so much that the tunnel will not stabilize without internal support pressure.

Fig. 7 shows the variation of excavation damage zone (R_d) with reduce of internal support pressure (P_i) at different brittleness parameters.

Fig. 7 can explain the spreading of the damage zone with decreasing internal support pressure. With decrease of fictitious inner support pressure, the excavation damage zone increases. The effect of brittleness parameter (b) on development of the damage zone (GRC) is illustrated in Fig. 7. It is shown in Fig. 7 that the excavation damage zone radius (R_d) increases with brittleness parameter increment at same inner support pressure (P_i). For $b = 3$, corresponding to a brittle rock, a substantial fracture zone will develop with no internal support pressure.

Hence, the damage zone of a tunnel excavated in a brittle rock is more than a less brittle rock if other rock strength properties are same. The different values of excavation damage radius calculated using different brittleness parameters illustrate the important effect of the brittleness on tunnel stability.

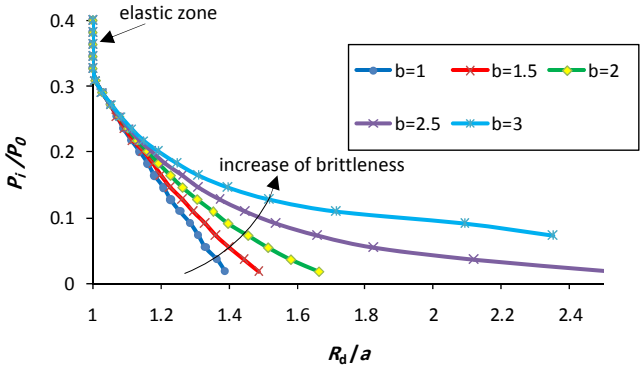

Fig. 7. Variation of damage zone radius with reduce of inner support pressure at different brittleness parameters

4.2. Stress distributions

Fig. 8 shows the development of radial stresses in the rock with distance from the tunnel wall at different brittleness parameters (b) with same inner support pressure ($P_i = 0$).

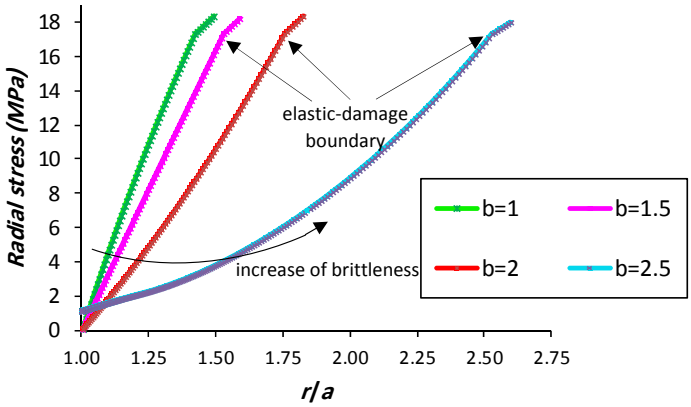

Fig. 8. The radial stress distributions in rock mass surrounding the tunnel

The radial stress increases with distance from the tunnel wall in damage zone and reaches a maximum at the elastic-damage boundary. The elastic-damage interfaces are shown in Fig. 8. The radial stresses in damage zone increases with greater rate than the elastic zone. With increment of brittleness parameters (b), the excavation damage zone increases so the radial stress raise rate in damage zone declines. Fig. 9 illustrates the tangential stresses distribution in the rock with distance from the tunnel wall at different brittleness parameters (b) with same inner support pressure ($P_i = 0$).

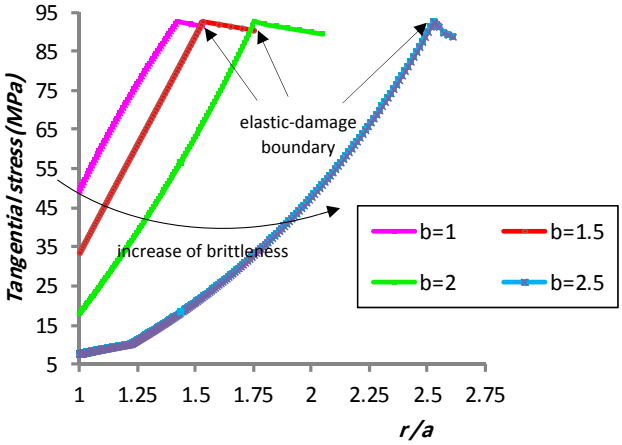

Fig. 9. The tangential stress distributions in rock mass surrounding the tunnel

It is evident in Fig. 9 that the tangential stress increase with distance from the tunnel wall in damage zone and reach a maximum value at the elastic-damage boundary. Following that the tangential stress decrease in elastic zone. In Fig. 9, the elastic-damage interfaces are illustrated. In Fig. 9, the tangential stress at tunnel wall decreases with brittleness increment because a more brittle rock cannot sustain high tangential stresses at post-peak region.

4.3. Convergence test

A principal strain increment of $d\varepsilon_{\theta(j)} = 0.01\varepsilon_{\theta(j-1)}$ is considered in this study as well as in Brown et al. (1983). In fact the value of strain increment is chosen arbitrarily. In order to check the convergence of the solution, the results of the radial displacements are compared for different values of strain increment 0.05, 0.02, 0.01, 0.005, 0.003, 0.002. Fig. 10 shows ground response curves at different values of strain increments.

In Fig. 10, good convergence of the ground response curves with different values of strain increments can be seen.

5. Conclusions

The conditions associated with complex rock openings are such that the rock material, acting as a quasi brittle material, damages and its stiffness modulus gradually degrade. According to different inner pressure, elastic and damage zones will be created around the tunnel. In this study a damage model was implemented into a convergence-confinement method (CCM). The numerical stepwise procedure was formulated based on the damage mechanics theory. The developed method was implemented to evaluate the ground response curve (GRC). The stress and displacement distributions were calculated in damage zone. The damage zone radius was estimated based on the damage mechanics.

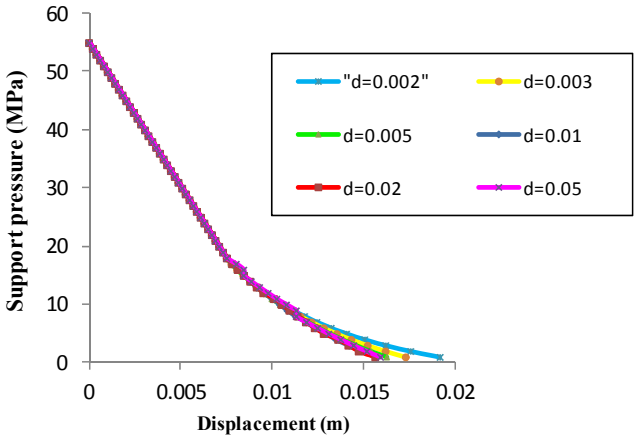

Fig. 10. Convergence test of GRCs with different values of strain increments

The analysis of results show the important effect of brittleness parameter on the tunnel wall convergence, ground response curve and excavation damage radius. The results show that the developed method has good capabilities in predicting damage region around tunnels. Additionally, the model input data can be determined more easily. In spite of successful application of the developed method, it is believed that it is still work in progress and needs further verification.

References

Alonso E., Alejano L., Varas F., Fdez-Manin G., Carranza-Torres C., 2003. *Ground reaction curves for rock masses exhibiting strain softening behavior*. Int. J. Numer. Anal. Meth. Geomech. 27 (13), 1153-1185.

Brown E., Bray J., Landayi B., Hoek E., 1983. *Ground response curves for rock tunnels*. ASCEJ. Geotech. Eng. Div. 109 (1), 15-39

Carol I., Rizzi E., Willam K., 2001. *On the formulation of anisotropic elastic degradation. I. Theory based on a pseudo-logarithmic damage tensor rate*. Int. J. Solids and Structures 38, 491-518.

Carranza-Torres C., Fairhurst C., 1999. *The elasto-plastic response of underground excavations in rock masses that satisfy the Hoek-Brown failure criterion*. Int. J. Rock Mech. Min. Sci. 36 (6), 777-809.

Detournay E., 1986. *Elastoplastic model of a deep tunnel for a rock with variable dilatancy*. Rock Mech. Rock Engng. 19, 99-108.

Guan Z., Jiang Y., Tanabasi Y., 2007. *Ground reaction analyses in conventional tunneling excavation*. Tunnelling and Underground Space Technology 22, 230-237.

Jiang Y., Yoneda H., Tanabashi Y., 2001. *Theoretical estimation of loosening pressure on tunnels in soft rocks*. Tunnelling and Underground Space Technology 16 (2), 99-105.

Lee Y.K., Pietruszczak S., 2008. *A new numerical procedure for elasto-plastic analysis of a circular opening excavated in a strain-softening rock mass*. Tunnelling and Underground Space Technology 23, 588-599.

Molladavoodi H., Mortazavi A., 2010. *Development of a damage model for rock materials under compressive and tensile stress fields*. Arch. Min. Sci., 55 (3), 637-668.

Molladavoodi H., Mortazavi A., 2011. *A damage-based numerical analysis of brittle rocks failure mechanism*. Finite Elements in Analysis and Design, 47, 991-1003.

Oreste P., Peila D., 1996. *Radial passive rockbolting in tunnelling design with a new convergence confinement model*. Int. J. Rock Mech. Min. Sci. Geomech. Abstr. 33 (5), 443-454.

Park K.H., Tontavanich B., Lee J.G., 2008. *A simple procedure for ground curve of circular tunnel in elastic-strain softening rock masse*. Tunnelling and Underground Space Technology, 23, 151-159.

Shao J.F., Chau K.T., Feng X.T., 2006. *Modeling of anisotropic damage and creep deformation in brittle rocks*. Int. J. Rock Mechanics & Mining Sciences. 43, 582-592.

Timoshenko S., Goodier J., *Theory of Elasticity*. McGraw-Hill, New York (1970).

Yazdani S., Schreyer H.L., 1988. *An anisotropic damage model with dilation for concrete*. Mechanics of Materials. 7, 231-244.

Zhu W.C., Tang A. 2004. *Micromechanical model for simulating the fracture process of rock*. Rock Mech. Rock Engng. 37(1), 25-56.

Received: 27 August 2012

APPENDIX
GROUND RESPONSE CURVE CALCULATION

Input data

f_{c0} = uniaxial compressive strength of rock, E, v = Young's modulus and Poisson's ratio of rock material, ϕ = friction angle of rock material, λ = re sidual coefficient, b = brittleness parameter, P_0 = in situ hydrostatic field stress, a = tunnel radius

Preliminary calculation

1. $G = \dfrac{E}{2(1+\nu)}\dfrac{1}{2}$
2. $k_\phi = \dfrac{1+\sin\phi}{1-\sin\phi}$
3. $\sigma_{r(1)} = \sigma_{re} = (2P_0 - f_{c0})/(1+k_\phi)$
4. $\sigma_{\theta(1)} = \sigma_{\theta e} = 2P_0 - (2P_0 - f_{c0})/(1+k_\phi)$
5. $\varepsilon_{r(1)} = \varepsilon^e_{r(1)} = \varepsilon_{re} = -(P_0 - \sigma_{r(1)})/(2*G)$
6. $\varepsilon_{\theta(1)} = \varepsilon^e_{\theta(1)} = \varepsilon_{\theta e} = (P_0 - \sigma_{r(1)})/(2*G)$
7. $\rho_{(1)} = \dfrac{r_{(1)}}{r_d} = 1$
8. $D_{(1)} = 0$

Sequence of calculation for each ring

9. $d\varepsilon_{\theta(j)} = 0.01\varepsilon_{\theta(j-1)}$

10. $\varepsilon_{\theta(j)} = \varepsilon_{\theta(j-1)} + d\varepsilon_{\theta(j)}$

11. If $\sigma_{\theta(j)} > f_{cr}$ then

11-1. $f_{c(j)} = \left(\frac{f_{c0}}{\varepsilon_{\theta e}}\right) \cdot \left(\frac{\varepsilon_{\theta e}}{\varepsilon_{\theta(j)}}\right)^{b} \cdot \varepsilon_{\theta(j)}$

11-2. $D_{(j)} = 1 - \left(\frac{\varepsilon_{\theta e}}{\varepsilon_{\theta(j)}}\right)^{b}$

12. If $\sigma_{\theta(j)} < f_{cr}$ then

12-1. $f_{c(j)} = f_{c0} \cdot \lambda$

12-2. $D_{(j)} = 1 - \frac{\lambda\varepsilon_{\theta e}}{\varepsilon_{\theta(j)}}$

13. $f_{(j)} = \acute{\imath} \,/\left(1 - D_{(j)}\right)$

14. $d\varepsilon_{r(j)} = d\varepsilon^{e}_{r(j-1)} - f \cdot (d\varepsilon_{\theta(j)} - d\varepsilon^{e}_{\theta(j-1)})$

15. $\rho_{(j)} = \frac{2\varepsilon_{\theta(j-1)} - \varepsilon_{r(j-1)} - \varepsilon_{r(j)}}{2\varepsilon_{\theta(j)} - \varepsilon_{r(j-1)} - \varepsilon_{r(j)}} \cdot \rho_{(j-1)}$

16. $\sigma_{r(j)} = \sigma_{r(j-1)} - 2\left(\frac{\rho_{(j-1)} - \rho_{(j)}}{2\rho_{(j)} + k_{\phi}\left(\rho_{(j-1)} - \rho_{(j)}\right)}\right) \cdot f_{c(j)}$

17. $\sigma_{\theta(j)} = k_{\varnothing} \cdot \sigma_{\theta(j)} + f_{c(j)}$

18. $\varepsilon^{e}_{r(j)} = \frac{1}{2G}\left[(1-\nu)\left(\sigma_{r(j)} - P_0\right) - \nu\left(\sigma_{\theta(j)} - P_0\right)\right]$

19. $\varepsilon^{e}_{\theta(j)} = \frac{1}{2G}\left[(1-\nu)\left(\sigma_{\theta(j)} - P_0\right) - \nu\left(\sigma_{r(j)} - P_0\right)\right]$

20. $d\varepsilon^{e}_{r(j)} = \varepsilon^{e}_{r(j)} - \varepsilon^{e}_{r(j-1)}$

21. $d\varepsilon^{e}_{\theta(j)} = \varepsilon^{e}_{\theta(j)} - \varepsilon^{e}_{\theta(j-1)}$

22. If $\sigma_{r(j)} > P_i$, then increase j by 1 and repeat calculation sequence for next ring.

23. If $\sigma_{r(j)} = \sigma_{r(n)} < P_i$, then calculate $\rho_{(n)}$ at tunnel radius (a)

24. $R_d = \dfrac{a}{\rho_{(n)}}$, $u_{(n)} = \varepsilon_{\theta(n)} \cdot a$